International Journal of Mechanical and Production Engineering Research and Development (IJMPERD)
ISSN (P): 2249-6890; ISSN (E): 2249-8001
Vol. 7, Issue 6, Dec 2017, 121-134

COMPUTATIONAL INVESTIGATION, ON THERMOHYDRAULIC CHARACTERIZATION OF LIQUID HYDROGEN AND LIQUID NITROGEN IN MICROCHANNELS

JEET PRAKASH SHARMA & AASHISH SHARMA

School of Mechanical Engineering, Lovely Professional University, Punjab, India

ABSTRACT

Due to increasing application of Micro-Electro-Mechanical Systems (MEMS), are in constant need of better and improved understanding of fluid flow and heat transfer characteristics, in micro channels. This paper offers a computational analysis, by using the FLUENT 14.0 and ICEM software. The purpose of this study is to explore, the Thermo-hydraulic traits of single-phase fluid flow by using air, liquid nitrogen, and liquid hydrogen as flowing fluids in smooth circular micro channels over the hydraulic diameter range from 1 µm to 100 µm. The mass flow rate varies from 0.001 kg/sec to 0.01 kg/sec for every particular diameter. The length of micro channel was kept constant as 0.1 meter. Flow in the micro channels was considered as turbulent and the variation in Reynolds number value for all three flowing fluids is considered to primarily examine the diversification in friction factor and nusselt number, over the diameter range. Leisurely contemplation is made to justify the parity of computational results from conventional theory, while friction factor and pressure drop was seen to be compatible with classical theory of fluid flow for all three flowing fluids.

KEYWORDS: Micro Channel, Liquid Nitrogen [LN_2], Liquid Hydrogen [LH_2], Pressure Drop, Turbulent Flow & Heat Transfer

Received: Sep 20, 2017; **Accepted:** Oct 12, 2017; **Published:** Nov 04, 2017; **Paper Id.:** IJMPERDDEC201713

Original Article

INTRODUCTION

The recent advancement in micro heat exchanger technology has pushed the thermal restriction in electronic [4].

This idea of implementing the microchannels, for quenching the heat emitted from very large-scale integration (VLSI) circuits was first proposed, by Tuckerman [5]. He expounded about the direct contact and cold plate hybrid technology, by exerting laminar flow of water in the microchannels and imbibing, 150 W/cm^2 of heat flux. The study carried out [6-8], to depict the flow and heat transfer characteristics of water flowing in the microchannels of hydraulic diameter, ranging from 130µm to 340µm. It was observed that, laminar heat transfer took place at Re=200-700 and fully turbulent convective heat transfer was achieved, at Re=400-1500.

In the experiment, performed [9-10] to investigate the flow characteristics in the microchannels, Isopropyl data demonstrated that, friction factor was not dependent of Re, but it was dependent on the size of the channel. However, in case of silicon oil, friction factor was independent of size of the channels, but it was merely dependent on the value of Re. The investigation conducted [11] for the liquid flow in round and square microchannels of hydraulic diameters, ranging 15–150 µm over a Reynolds number range of 8–2300 and it was seen that, there was

no distinguishable deviation from stokes theory, which suggests that, the flow in microchannels strongly can be predicted by the conventional theory.

Study conducted on two phase pressure drop, in horizontal circular microchannel [12] having hydraulic diameter 781μm showed that, Two phase pressure drop increases linearly with heat flux and vapour friction, for both R134a and R245fa refrigerants. Another study [13] performed an Experimental and Numerical Study, of Flow and Heat Transfer in Trapezoidal Microchannels. It was indicated that, for a particular pumping power, if heating power is increased at the substrate, the thermal resistance decreases, however the sub-thermal resistance proportion is nearly unchanged.

Amirah et al. [23], investigated the effects of hydraulic diameter and aspect ratio, in flow and heat transfer in microchannels. The range of hydraulic diameters was 0.1–1 mm and the aspect ratio was kept 1. Reynolds number ranger was 100-2000. Results of the study suggested that, friction factor decreases with the aspect ratio, greater than 2 and also found that; aspect ratio doesn't affect the heat transfer co-efficient. Another study conducted by Omer et al. [24], to investigate the conjugate heat transfer performance of a heat sink. Results predicted significant increase in heat transfer but secondary flow was observed to be blocking the heat transfer. In an another investigation conducted by Seyed Ebrahim Ghasemi et al. [25], investigated the heat transfer performance of a heat sink, used for the cooling of electronic applications. In this experiment, the main channel of hydraulic diameter 4 mm, 6 mm, 8 mm was investigated. Results of the study suggested that, the heat sink having D_h= 4 mm has much lower thermal resistance, than the rest and increase in diameter decreases in pressure drop.

TRANSITION TO TURBULENCE

Conventional theory suggests that when Reynolds number increases to a certain value the fluid flow in duct displays an astonishing transition from laminar flow in to turbulent flow. The cause of generation of turbulence in flow is eddies formation due to high fluid velocity. The fluid flow inside a smooth pipe having uniform cross-section and low Reynolds number results fluid particles to move along the streamline. According to the Newton's law, viscous forces try to slowdown the particle near to the wall. The flow is in well order and called as laminar flow. However, at higher Reynolds number this well ordered flow cease to exist and mixing of particle from different layers starts. The fluctuation in fluid velocity at point causes momentum exchange in transverse direction. The transition from laminar to turbulent is huge in flow resistance pattern.

The basic governing equations [14] are,

- **Continuity equation**

$$\rho_l \nabla . U = 0 \tag{1}$$

- **Momentum equation**

$$\rho_l (U . \Delta U) = -\nabla P + \nabla . (\mu_l \nabla U) \tag{2}$$

- **Energy equation**

$$\rho_l c_{p,l} (U . \nabla T) = k_l \nabla^2 T \tag{3}$$

A study performed on general boundary condition for liquid flow at solid surfaces [15] provided the molecular dynamics simulations to calculate the slip-flow boundary condition dependence on shear rate.

$$\Delta u_w = u_{fluid} - u_{wall} = L_s \frac{\partial u}{\partial y} \quad (4)$$

Where, L_s is fixed length of slip, and $\frac{\partial u}{\partial y}$ is the rate of strain at the wall. The objective of Thompson and Troian's numerical analysis was to quantify the ascendancy of slip at a solid-liquid interface, as the interfacial parameters and the change in shear rate.

RESULTS AND DISCUSSIONS

Present 2-D computational study on Thermohydraulic characterization, was performed to observe the behaviour of fluid flow and heat transfer parameters, in microchannels. In the investigation, the microchannels of varying diameter from 1µm to 100µm, were modelled as keeping the length 0.1 meter constant. The air, liquid nitrogen and liquid hydrogen were chosen as flowing fluids. For every diameter, a wide range of mass flow rate, from 0.5 gram/sec to 10 gram/sec were used for the analysis of fluidic and thermal characteristics.

This study is based on following assumptions.

- Flow in microchannel is turbulent.
- Slip at the wall is zero (no slip).
- Axi-symmetric condition.

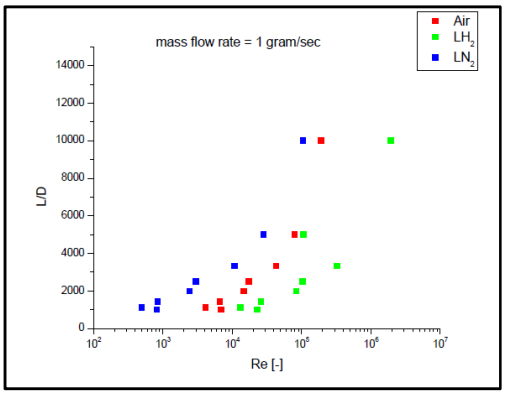

Figure 1: Comparison of Dimensional Entrance Length of Air, Liquid Hydrogen and Liquid Nitrogen at Constant Mass Flow Rate

Hydraulic Characteristics

Entrance Length

The graphs for the numerical dimensional entrance length vs. Reynolds number in the figure 1, was plotted for the hydraulic diameter range of 1µm to 100µm over the constant mass flow rate of 1 gram/sec for the comparison of three flowing fluids as air, liquid hydrogen and liquid nitrogen for circular geometry of the microchannels. Fluid flow velocity at inlet was considered to be uniform. According to the figure 1, the dimensional entrance length does not have significant impact for the increasing value of diameter and it was seen to be getting independent of the diameter as well for all three fluids.

Friction Factor

For fluid flow in microchannel at constant mass flow rate, pressure gradient $\frac{\Delta P}{\Delta l}$is required to drive the liquid.

The co-efficient of flow resistance f is known as friction factor and it is related to the Reynolds number by Blasius equation for turbulent flow,

$$f = 0.3164(Re)^{0.25} \quad (5)$$

The Blassius Equation gives the friction factor for turbulent flowing smooth pipes for $Re \leq 10^5$ [16].

For fully developed laminar flow at macroscale in pipe can be written as,

$$f = \frac{64}{Re} \quad (6)$$

and,

$$Re = \frac{\rho v D}{\mu} \quad (7)$$

From conventional theory, the product of the Reynolds number and friction factor,$Re \times f = C$ the value of C=64 for circular pipe flow.

Table 1: Friction Factor Co-Relations for various Geometrical Configurations [17]

Rectangular	**Friction factor**
a/b=1	56.92/Re
a/b=2	62.20/Re
a/b=3	68.36/Re
a/b=4	72.92/Re
a/b=6	78.80/Re
a/b=8	82.32/Re
Triangular	----------
A=30˚	52.28/Re
A=60˚	53.32/Re
A=90˚	52.60/Re
A=120˚	50.96/Re

Shah and London correlation [18] can be applied for laminar flow for both conditions whether flow has reached fully developed state or not at the outlet.

$$f_L Re_{avg} = \sqrt{\left[\frac{3.2}{\{L/(D*Re)\}^{0.57}}\right]^2 + (fRe)^2} \quad (8)$$

Where,

$$fRe = 96(1 - 1.3553a + 1.9467a^2 - 1.7012a^3 + 0.9564a^4 - 0.2537a^5) \quad (9)$$

The reliability of the above correlations has been validated by the recent experimental work of Investigation of liquid flow in microchannels [19].

The effects of friction factor and the pressure drop, for single phase flow in microchannels, over the hydraulic diameter range of 1µm to 100µm over the mass flow rate range of 0.5 gram/sec to 10 gram/sec are discussed. According to the Blassius equation for friction factor, $f = 0.3164Re^{-0.25}$ defines the dependence of friction factor, over the Reynolds number for turbulent flow.

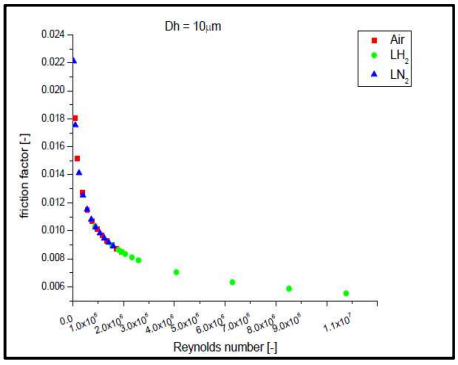

Figure 2: Plot of Friction Factor vs. Reynolds Number for Dh = 10µm

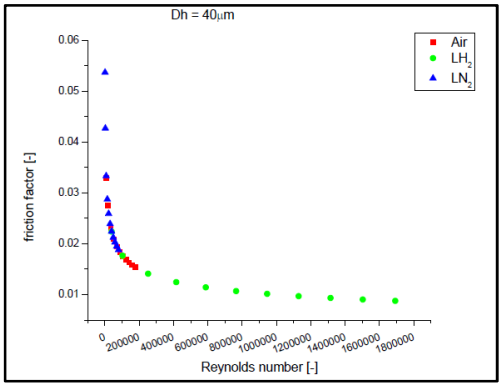

Figure 3: Plot of Friction Factor vs. Reynolds Number for Dh = 40µm

The above figure 2, shows the variation in friction factor, with respect to Reynolds number for 10µm diameter however, the figure 3 shows the variation for 40µm diameter. The behaviour of friction factor characteristic for air, liquid nitrogen and liquid hydrogen is compared and seen that, as the value of Reynolds number increases, the value of friction factor for all three flowing fluids decreases. It can be seen further for both cases that the liquid nitrogen displays the highest value of friction factor and liquid hydrogen displays the lowest value of friction factor among all three fluids. One important observation was also made that as the hydraulic diameter was increased for constant mass flow rate, the value of friction factor was increased. It also can be observed from the figures that the variation in friction factor occurs as the conventional channels on the basis of moody chart and comes in completely in agreement with conventional behaviour for friction factor.

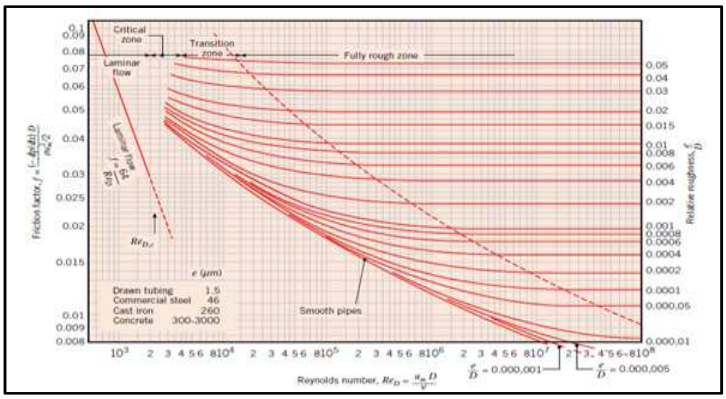

Figure 4: Moody's Diagram

Above given moody chart in figure 4 depicts the behaviour of fluid flow according to the conventional theory and it shows that for turbulent flow, the variation of friction factor follows a curve in decreasing order as the value of Reynolds number keep increasing and same behaviour is followed by the air, liquid nitrogen and liquid hydrogen thus it can be conclude on the safe side that fluid flow behaviour in microchannels, does follows the conventional theory.

Pressure Drop

Basically, there are three major components, which have their contribution to the overall pressure drop in fluid flow, in microchannels or duct. The losses at inlet and exit need to be quantified as the flow in microchannels takes place. While, evaluating the hydrodynamic developing length care must be taken into account. Finally, the rest of the length will have the fully developed frictional loss. The components of the total pressure drop, can be seen in the following given equation [21].

$$\Delta p = \frac{\rho V^2}{2}\left[\kappa i + \kappa o + \frac{f_{app} L}{D}\right] \tag{10}$$

The co-efficient of inlet and outlet loss are represented by κ_i and κ_o. However, The Navier–Stokes (NS) equation can be simplified, in terms of Hagen-Poiseuille equation and the feature of Pressure drop, for the circular pipe flow, according to the conventional theory can be described as,

$$\Delta P = \frac{128 \mu L Q}{\pi D^4} \tag{11}$$

Where D and L, are the diameter and the length of the microchannel, respectively, ΔP is the pressure drop amidst the two ends of the microchannel, and μ is the viscosity of the fluid. This equation is valid for laminar regime, as well as turbulent regime for incompressible flow.

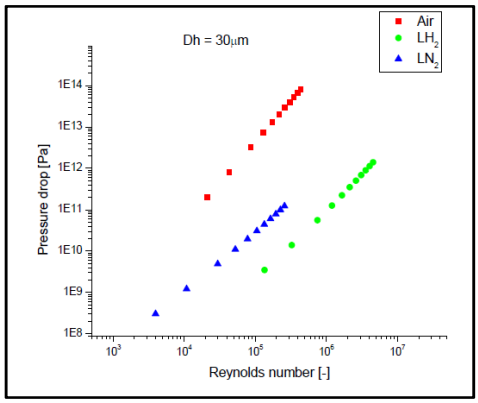

Figure 5 : Plot against Pressure Drop and Reynolds Number, Dh= 30μm

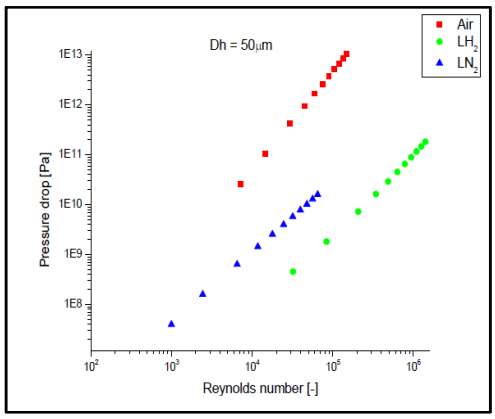

Figure 6: Plot against Pressure Drop and Reynolds Number, Dh= 50µm

In the above figure 5, the behaviour of pressure drop, for flowing liquid air, liquid nitrogen and liquid hydrogen for hydraulic diameter 30 µm and in the figure 6, the behaviour for hydraulic diameter 70µm is shown. From the above figures, it can be seen that, as the value of Reynolds number for particular hydraulic diameter is increased, with the increasing value of mass flow rate, the value of pressure drop, also keep on increasing for all flowing fluids. As a result, it can be predicted that, by pressure drop being the function of mass flow rate, according to Bernoulli equation,

$$(P_1 - P_2) = \frac{\rho}{144}[(Z_2 - Z_1) + \frac{(V_2^2 - V_1^2)}{2g} + H_L \quad (13)$$

It was also observed that, as the hydraulic diameter was increased at constant mass flow rate, the value of pressure drop decreased for all three flowing fluids. Both figures demonstrate that, for every diameter air yields the highest value of pressure drop and liquid nitrogen yields, the lowest value.

In the figure 7, a graph shows a variation in pressure drop against mass flow rate for different hydraulic diameters. This graph also shows that as the value of mass flow rate increases, the pressure drop increases for all considered diameters. However, it also can be seen that as the hydraulic diameter increases, the pressure drop decreases and the microchannel, having hydraulic diameter of 1µm shows the least value of pressure drop, among the considered diameters.

Wall Shear Stress

When the fluid moves along the solid boundary, it offers some resistance force, which reduces the velocity of the fluid; however, the viscosity plays the role of an important factor.

$$\mu = \frac{\tau}{\frac{\partial u}{\partial y}} \quad (13)$$

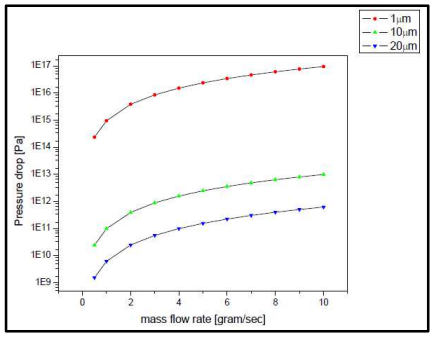

Figure7: Plot against Pressure Drop and Mass Flow Rate

No slip phenomenon is defined, when wall boundary does not offer any resistance to the fluid motion, thus fluid will flow without friction at the wall contact.

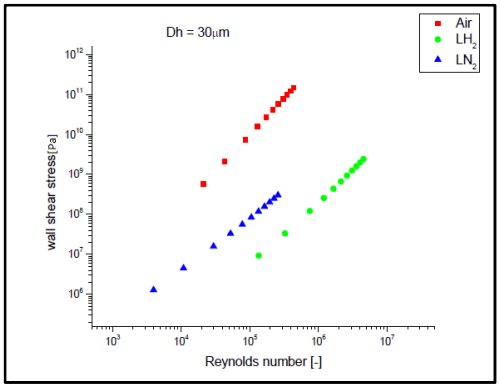

Figure 8: Plot of Wall Shear Stress and Reynolds Number, Dh= 30µm

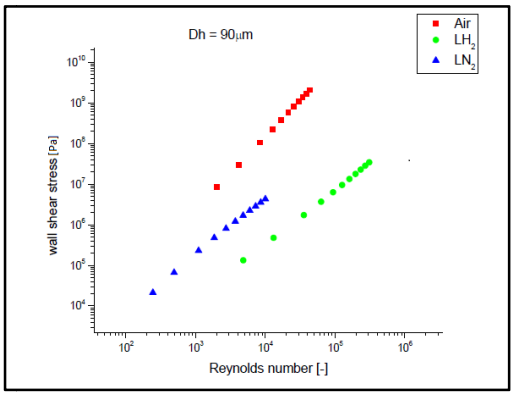

Figure 9: Plot of Wall Shear Stress and Reynolds Number, Dh= 90µm

In the above given figure 8, it shows the effect of increasing value of Reynolds number, over the wall shear stress for hydraulic diameter of 30µm and figure 9, shows the graph for 90µm, for the varying mass flow rate. Both figures show that, as the value of mass flow rate increases, Reynolds number increases and with the increasing value of Reynolds number, the value of wall shear stress increases. It is also observed that, as the hydraulic diameter increases, wall shear stress is decreases. Both figures show that, the air yields the highest value of the wall shear stress and liquid nitrogen yields the lowest value of wall shear stress.

Heat Transfer Characteristics

Rate of Heat Transfer

Heat transfer by means of convection process, provides a mode of transferring the heat between fluid to fluid or fluid to solid, quickly from the exchange surface. Fluids used in the systems and processes; incur the changes in their thermal state in heat exchanger. The basic equation for heat transfer by convection is,

$$q = hA(T_s - T_f) \tag{14}$$

However, when a cold fluid is flowing in a hot channel with a solid-liquid temperature difference, the heat transfer between the liquid and solid at boundary takes place. From conservation of energy, the rate of heat transfer imbibe by the liquid results in a liquid's temperature increase,ΔT_i

$$q = mc_p\Delta T_i \quad (15)$$

Where, m is the mass flow rate of fluid and c_p isspecific heat of the liquid.

According to the conventional theory, the heat transfer co-efficient, is unswayed by the Reynolds number in the fully developed region of laminar flow is given by,

$$h = \frac{Nu \times k}{D} \quad (16)$$

The nusselt number for the flow in microchannel, can be calculated by Chilton-Colburn analogy [22] given as,

$$Nu = 0.125 f Re \times Pr^{0.33} \quad (17)$$

The local convective heat transfer coefficient and local Nusselt number [22] are expounded as,

$$h_x = \frac{qA}{\mathrm{N}\, A_{ch}(T_{w,x} - T_x)} \quad (18)$$

According to the conventional theory, the heat transfer characteristics in laminar flow for circular duct, can be expressed in terms of nusselt number, which is $Nu = \frac{hL}{k}$, *Nu = 4.36* [T_s= cons.] and *Nu= 3.66* [q''= cons.] [22].

However, for gas flow in circular channels, the value of nusselt number depends upon the Reynolds number, as follows,

Table 2: Nusselt Number Correlation for different Ranges of Reynolds Number [22]

Nusselt Number	Reynolds Number Range [Gas Flow]
$Nu= 0.989Re^{0.330}Pr^{0.33}$	Re=0.4-4
$Nu= 0.911Re^{0.385}Pr^{0.33}$	Re=4-40
$Nu= 0.683Re^{0.466}Pr^{0.33}$	Re=40-4000
$Nu= 0.193Re^{0.618}Pr^{0.33}$	Re=4000-40,000

Table 3: Nusselt Number Co-Relations for various Geometrical Configurations for Constant Surface Temp and Constant Surface Heat Flux [22]

Rectangular	T_s= Constant	q_s= Constant
a/b=1	Nu=2.96	Nu=3.61
a/b=2	Nu=3.39	Nu=4.12
a/b=3	Nu=3.96	Nu=4.79
a/b=4	Nu=4.44	Nu=5.33
a/b=6	Nu=5.14	Nu=6.05
a/b=8	Nu=5.60	Nu=6.49
Triangular	----------	----------
A =30˚	Nu=2.26	Nu=2.91
A =60˚	Nu=2.47	Nu=3.11
A =90˚	Nu=2.34	Nu=2.98
A=120˚	Nu=2.00	Nu=2.68

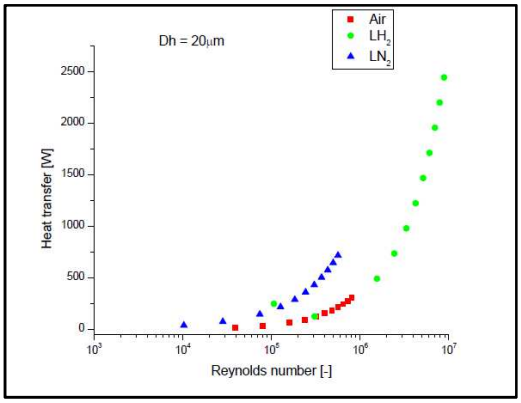

Figure 10: Plot against Heat Transfer and Reynolds Number, Dh= 20µm

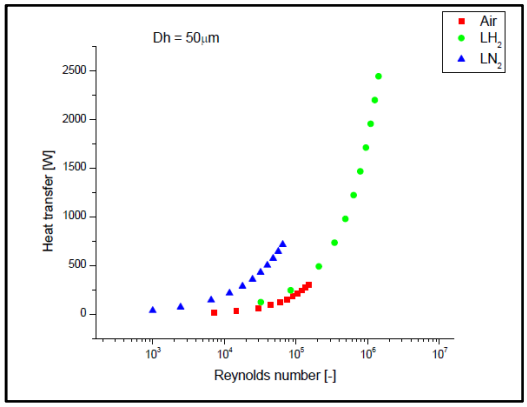

Figure 11: Plot against Heat Transfer and Reynolds Number, Dh= 50µm

In the below given figure 10 and figure 11, the graph for the hydraulic diameters 20µm and 50µm, respectively, shows the effects of Reynolds number variation, over the surface heat transfer. It can be observed from the given graphs, for hydraulic diameters that, as the value of Reynolds number increases with the increasing value of mass flow rate, the values of surface heat transfer increases. It was observed that, the liquid hydrogen yield the highest value of heat transfer and air yield the lowest value of heat transfer, among the all three flowing fluids. It also can be seen for the given both graphs that, as the value of hydraulic diameters increases, the value of heat transfer also increases but the increase in heat transfer is not so significant. These graphs also indicate that, liquid hydrogen and liquid nitrogen, being the cryogenic fluids show astonishing heat dissipation properties, when they are combined with microchannels. It also can be hoped that, they will be extremely useful tool in the area of microelectronics, for the purpose of eliminating the thermal restrictions, in order to enhance the performance of electronic instrument, as well as in the implementation in the area of cooling of turbine blades.

Nusselt Number

For the analysis of heat transfer characteristics, Nusselt number is the best and most important factor, which can be taken into consideration. Nusselt number is dimensionless number, which defines the dependence of heat transfer co-efficient of to the diameter of the duct and heat transfer co-efficient, shows the effects over the heat flux or the rate of heat transfer.

$$Nu = \frac{hD}{k} \tag{19}$$

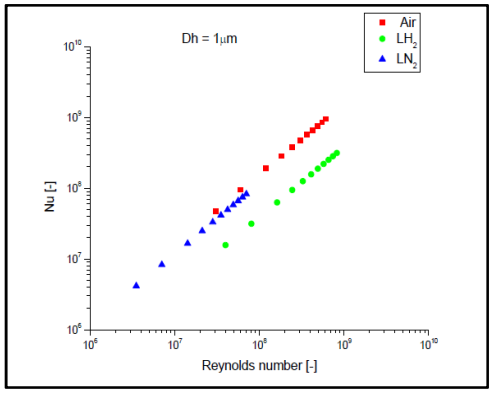

Figure 12: Plot of Nusselt Number and Reynolds Number, Dh= 1µm

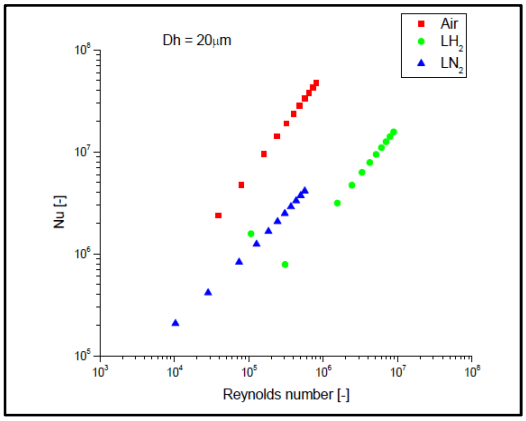

Figure 13: Plot of Nusselt Number and Reynolds Number, Dh= 20µm

The above given Figure 11 for the hydraulic diameter 1µm and figure 12 for hydraulic diameter of 20µm, explains the effects of Reynolds number, over the Nusselt number. It can be observed from the graphs that, as the Reynolds number value increases with the increasing value of mass flow rate, the value of Nusselt number also increases. Figures show that, by increasing the Reynolds, the Nusselt number increases however, on comparing the both figures it also can be observed that, for a particular value of mass flow rate if hydraulic diameter of the microchannel is increased, and the value of Nusselt number decreases. Both figures depicts that, the air yield the highest value of nusselt number in microchannels and the liquid nitrogen, yields the lowest value for the nusselt number, for all the considered diameters.

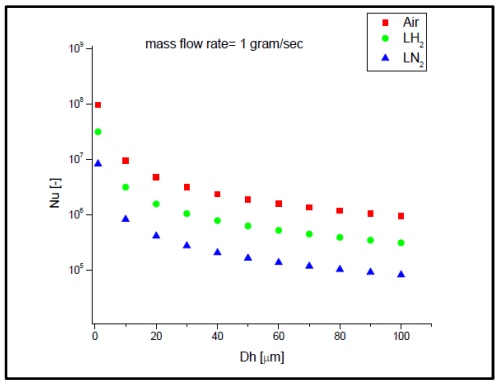

Figure 14: Plot against Nusselt Number and Hydraulic Diameters

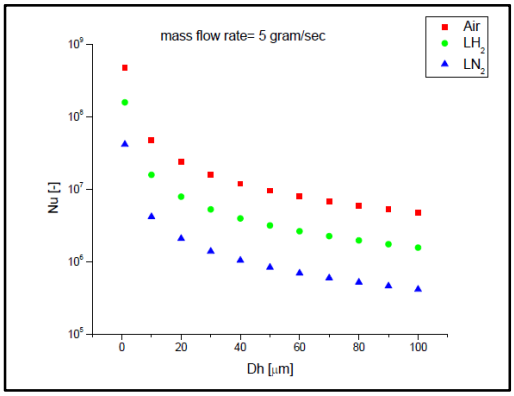

Figure 15: Plot against Nusselt Number and Hydraulic Diameters

Figure 14 is a graph drawn between the nusselt number and the hydraulic diameter, range from 1µm to 100µm. This graph depicts that, as the diameter of the microchannels increases, the value of nusselt number continue to decrease, while mass flow rate was kept constant. It also shows that, the air yields the highest value of nusselt number and the liquid nitrogen, yields the lowest value of nusselt number, among all three flowing fluids. Same kind of behaviour can be seen from the figure 15. However, on comparing the both graphs it can be seen that, as the mass flow rate is increased, the value of nusselt number also gets higher.

CONCLUSIONS

In this paper, a computational investigation to understand the Thermohydraulic characteristics in microchannels by considering air, liquid nitrogen and liquid hydrogen, as flowing fluid was carried out. For single-phase flow and turbulent flow regime, the fluid flow characteristics, in microchannels with hydraulic diameter range of 1µm to 100µm, obeys the classical flow theory. The friction factor behaviour, for all three flowing fluids at varying mass flow rate in the range of 0.5 gram/sec to 10 gram/sec, follows the same as for the conventional channel, as seen according to the moody diagram. Pressure drop was found to be increasing, with increasing Reynolds number. It was observed that, wall shear stress increases with increasing value of Reynolds number and follows shear thinning behaviour. In the case of heat transfer characteristics, as the Reynolds number increased with increasing value of mass flow rate, the rate of heat transfer was also increasing. It was seen that nusselt number, increasing with increasing Reynolds number for all three flowing fluids. It was observed that, with the use of cryogenic fluids such as liquid nitrogen and liquid hydrogen, the heat removal capacity of microchannels can be increased sufficiently, so it could be employed in the turbine blades and vanes as a substitute of cooling technique.

REFERENCES

1. *G Hetsroni, AMosyak, Z Segal, & G Ziskind. A uniform temperature heat sink for cooling of electronic devices. International Journal of Heat and Mass Transfer; 45(16), pp. 3275-3286, 2202.*
2. *S. L Qi, P Zhang, R. Z Wang, & L. X Xu. Flow boiling of liquid nitrogen in micro-tubes: Part II–Heat transfer characteristics and critical heat flux. International Journal of Heat and Mass Transfer; 50(25),pp. 5017-5030, 2007.*
3. *J Koo, & C Kleinstreuer. Viscous dissipation effects in microtubes and microchannels. International Journal of Heat and Mass Transfer; 47(14), pp. 3159-3169, 2004*
4. *A. M Sahar, M. R Özdemir, E. M Fayyadh, J Wissink, M. M Mahmoud & T. G Karayiannis. Single phase flow pressure drop*

and heat transfer in rectangular metallic microchannels. Applied Thermal Engineering; 93,pp. 1324-1336, 2016.

5. *D. B Tuckerman & R. F. W Pease. High-performance heat sinking for VLSI. IEEE Electron device letters; 2(5), pp.126-129, 1981.*
6. *B. X Wang & X. F Peng. Experimental investigation on liquid forced-convection heat transfer through microchannels. International Journal of Heat and Mass Transfer; 37,pp. 73-82, 1994.*
7. *X. F Peng & G. P Peterson. Forced convection heat transfer of single-phase binary mixtures through microchannels. Experimental Thermal and fluid science;12(1), pp. 98-104, 1996.*
8. *X. F Peng, G. P Peterson, & B. X Wang. Frictional flow characteristics of water flowing through rectangular microchannels. EXPERIMENTAL HEAT TRANSFER. An International Journal;7(4),pp. 249-264, 1994.*
9. *J Pfahler, J Harley, H Bau, & J Zemel. Liquid transport in micron and submicron channels. Sensors and Actuators A: Physical; 22(1-3), pp. 431-434, 1990.*
10. *J Pfahler, J Harley, H Bau, and J. N Zemel. Gas and liquid flow in small channels. Micromechanical Sensors, Actuators, and Systems; 32, pp.49-58, 1991.*
11. *J Judy, D Maynes, & B. W Webb. Characterization of frictional pressure drop for liquid flows through microchannels. International Journal of heat and mass transfer: 45(17), pp. 3477-3489, 2002.*
12. *R Ali, B Palm, & M. H Maqbool. Experimental investigation of two-phase pressure drops in a microchannel. Heat Transfer Engineering; 32(13-14), pp. 1126-1138, 2011.*
13. *L Chai, G Xia, & J Qi. Experimental and numerical study of flow and heat transfer in trapezoidal microchannels. Heat Transfer Engineering; 33(11), pp. 972-981, 2012.*
14. *Z Li, W. Q Tao, & Y. L He. A numerical study of laminar convective heat transfer in microchannel with non-circular cross-section, A preliminary version of this paper was presented at ICMM05: Third International Conference on Microchannels and Mini-channels, held at University of Toronto, June 13–15, 2005, organized by SG Kandlikar and M. Kawaji, CD-ROM Proceedings, ISBN: 0-7918-3758-0, ASME, New York. International journal of thermal sciences: 45(12), 1140-1148, 2006.*
15. *P. A Thompson, & S. M Troian. A general boundary condition for liquid flow at solid surfaces. Nature; 389(6649), pp. 360-362, 1997.*
16. *G. M Mala & D Li. Flow characteristics of water in microtubes. International journal of heat and fluid flow; 20(2), pp. 142-148, 1999.*
17. *A. Y Çengel. External Forced Convection. Heat and Mass Transfer; pp. 367–418, 2002.*
18. *J. Y Jung & H. Y Kwak. Fluid flow and heat transfer in microchannels with rectangular cross section. Heat and Mass Transfer; 44(9), pp.1041-1049, 2008.*
19. *D Liu & S. V Garimella. Investigation of liquid flow in microchannels. Journal of Thermo physics and heat transfer; 18(1), pp. 65-72, 2004.*
20. *T. L Bergman, F. P Incropera, D. P DeWitt, and A. S Lavine. Internal flow, Fundamentals of heat and mass transfer. John Wiley & Sons; pp. 518-569, 2011.*
21. *M. E Steinke & S. G Kandlikar. Single-phase heat transfer enhancement techniques in micro channel and mini channel flows. InASME 2004 2nd International Conference on Micro channels and Mini channels; (pp. 141-148), 2004. American Society of Mechanical Engineers.*

22. *A. Y Çengel. Internal Forced Convection. Heat and Mass Transfer; pp. 419–458, 2002.*

23. *A. M Sahar, J Wissink, M. M Mahmoud, T. G. Karayiannis,& M. S. A Ishak,. (2017). Effect of Hydraulic Diameter and Aspect Ratio on Single Phase Flow and Heat Transfer in a Rectangular Microchannel. Applied Thermal Engineering.*

24. *O. B Kanargi, P. S. Lee and C Yap. A numerical and experimental investigation of heat transfer and fluid flow characteristics of a cross-connected alternating converging–diverging channel heat sink. International Journal of Heat and Mass Transfer, 106, pp.449-464, 2017.*

25. *S. E Ghasemi, A. A Ranjbar and M. J Hosseini. Experimental and numerical investigation of circular mini channel heat sinks with various hydraulic diameters for electronic cooling application. Microelectronics Reliability, 73, pp.97-105, 2017.*